Steel and Composite Structures, *Vol. 29, No. 5 (2018) 569-578*
DOI: https://doi.org/10.12989/scs.2018.29.5.569

Transient vibration analysis of FG-MWCNT reinforced composite plate resting on foundation

Puneet Kumar * and J. Srinivas [a]

Department of Mechanical Engineering, National Institute of Technology Rourkela, Rourkela-769008, India

(*Received September 24, 2017, Revised September 11, 2018, Accepted November 16, 2018*)

Abstract. This paper aims to investigate the transient vibration behavior of functionally graded carbon nanotube (FG-CNT) reinforced nanocomposite plate resting on Pasternak foundation under pulse excitation. The plate is considered to be composed of matrix material and multi-walled carbon nanotubes (MWCNTs) with distribution as per the functional grading concept. The functionally graded distribution patterns in nanocomposite plate are explained more appropriately with the layer-wise variation of carbon nanotubes weight fraction in the thickness coordinate. The layers are stacked up in such a way that it yields uniform and three other types of distribution patterns. The effective material properties of each layer in nanocomposite plate are obtained by modified Halpin-Tsai model and rule of mixtures. The governing equations of an illustrative case of simply-supported nanocomposite plate resting on the Pasternak foundation are derived from third order shear deformation theory and Navier's solution technique. A converge transient response of nanocompiste plate under uniformly distributed load with triangular pulse is obtained by varying number of layer in thickness direction. The validity and accuracy of the present model is also checked by comparing the results with those available in literature for isotropic case. Then, numerical examples are presented to highlight the effects of distribution patterns, foundation stiffness, carbon nanotube parameters and plate aspect ratio on the central deflection response. The results are extended with the consideration of proportional damping in the system and found that nanocomposite plate with distribution III have minimum settling time as compared to the other distributions.

Keywords: transient response; pasternak foundation; layer-wise formulation; weight fractions; functional grading

1. Introduction

Due to the great degree appealing properties, carbon nanotubes (CNTs) have been progressively viewed as a standout material in nanotechnology. The blend of CNTs and a polymer material result in nanocomposites of high specific strength and stiffness. Such properties make them to use in weight critical applications in aerospace and space technology. The embedded CNTs in polymer matrix specifically influence the mechanical performance of the composite structures. Over the last two decade, a wide range of investigations on the constitutive and material characterization of carbon nanotube reinforced composite (CNTRC) materials have been carried out (Kumar and Srivastava 2016, Kumar and Srinivas 2014, Seidel and Lagoudas 2006). Recent interest of research community towards tailor the properties of the matrix with help of fiber distribution emphasized on the concept of functionally graded composites. In same line, functionally graded carbon nanotube reinforced composite (FG-CNTRC) structures are required more attention so as to utilize the extraordinary properties of CNTs (Udupa *et al*. 2012).

FG-CNTRC plate and shell structures are having various applications in engineering fields and needs a detailed investigation in terms of static and dynamic characteristics under actual loading conditions. Several studies reported multitude of static and dynamic analysis works related to bending, free vibration and buckling behavior of FG-CNTRC structures (Chavan and Lal 2017, Wattanasakulpong and Chaikittiratana 2015, Zhang *et al*. 2017, Shokravi 2017).

Multiple references to the transient as well as forced analyses of laminated and functionally graded materials (FGM) plates can be found in earlier work (Wang *et al*. 2001, Kazanci 2009, Ebrahimi and Habibi 2017). A nonlinear dynamic study of FGM plates was conducted by Hao *et al*. (2010) to investigate the combined effect of transverse and in-plane excitations. Malekzadeh and Monajjemzadeh (2013) employed the finite element analysis along with Newmark's time integration to investigated the dynamic response of FGM plate under moving load and temperature simultaneously. Najafi *et al*. (2016) studied the dynamic response of conventional FG-plate under low velocity impact and examine the effect of nonlinear foundation, impactor's parameters and thermal field. The transient analysis of FG plates is extended for FG-CNTRC plate using a numerical strategy by Ansari *et al*. (2015). In this work, Galerkin solution based approach was employed to determine the nonlinear response by considering von Kármán-type kinematic relations. Lei et al. (2015) performed a time history analysis of an elasto-dynamic problem of FG-CNTRC plate. They found that volume fraction of CNT, plate aspect ratio, boundary

*Corresponding author, Ph.D. Student,
E-mail: puneetahalawat2009@gmail.com
[a] Associate Professor

ISSN: 1229-9367 (Print), 1598-6233 (Online)

conditions and CNT distribution highly influenced the dynamic response. Guo and Zhang (2016) worked on nonlinear resonant response of CNT reinforced plate and analyzed the time dependent behavior under combined parametric and forcing excitations. Ansari and Gholami (2016) predicted the nonlinear primary resonance of FG-CNTRC plate by employing Reddy's shear deformation theory and generalized differential quadrature technique. Moreover, Zhang *et al*. (2016) presented an elasto-dynamic analysis of FG-CNTRC quadrilateral plate using element-free approach and computed the response under a sudden dynamic load in transverse direction. An isogeometric model was developed by Phung-Van *et al*. (2015, 2017a, b) and integrated with the higher order shear deformation theory to obtain the nonlinear transient response of functionally graded nanoplates. *Jangam et al*. (2016) investigated the damping behavior of MWCNT/polymer composite and observed that aligned CNT reinforced nanocomposite samples show 37% improvement in structural damping compared to randomly oriented one. Swain *et al*. (2017) analyzed the impulse and frequency response of FG-CNT reinforced hybrid composite shell structure by considering Rayleigh damping. Few other studies on forced vibration response of FG-CNTRC structures were carried out under low velocity impact (Bayat *et al*. 2016) and periodic load (Moradi-Dastjerdi and Momeni-Khabisi 2017). Damped and control dynamic response of piezo-laminated CNT reinforced composite plate instrumented with nonlinear controller was presented using finite element method (Sharma *et al*. 2016). Feng *et al*. (2017) observed that the layer-wise variation of fiber volume/weight fraction provides more precise modeling of functionally graded moderately thick structure as it generates more accurate stress and strain-fields representation in discrete layers. In this line, a dynamic analysis of graphene platelet-reinforced composite plate is conducted using the concept of layer-wise variation of fiber weight fraction (Feng *et al*. 2017, Song *et al*. 2017). Recently, Tahouneh (2017) employed the modified Halpin-Tsai model to compute the material properties of CNT reinforced composite and free vibration characteristics has been evaluated for FG-CNT composite plate with various distributions. It appears that there is a scope for transient analysis of FG-CNT nanocomposite structures modeled with layer wise distribution and modified Halpin-Tsai model based on available literature.

In present work, transient vibration analysis of functionally graded MWCNT-reinforced polymer composite plate with simply-supported boundary condition is presented using Reddy's third-order shear deformation theory. The equations of motion for in-plane and out-of-plane directions are obtained by utilizing the Hamilton's principle. Modified Halpin-Tsai model, which is formulated using existing experimental data is employed for estimate the material properties. A proportional damping is also introduced in governing equations to account the energy dissipation. The Navier's approximate method is employed to acquire the time dependent algebraic equations. Further, the distributed transient pulse loads on the top face of the plate are considered and the central deflection response is obtained from Runge-Kutta fourth-order explicit time integration method. Effects of parameters such as the nanotube weight fraction, length of nanotube, their distributions, plate aspect ratio, damping coefficient and foundation stiffness parameters on the dynamic characteristics of FG-CNTRC plates are illustrated. Time-domain response characteristics under varying parameters are described in detail. The paper is organized as follows: section-2 described the layer-wise variation of weight fraction and mathematical modeling of the dynamic plate problem. Also, solution methodology is explained for simply support boundary conditions. Section-3 deals with numerical results and discussion and finally conclusions drawn from analysis are listed.

2. Problem statement and mathematical formulation

A multi-walled carbon nanotube reinforced composite square plate with thickness h, length a and width b is considered and multi-walled carbon nanotube is abbreviated as CNT throughout the analysis. The z-coordinate is taken along the thickness direction of the plate while x and y coordinates are taken along the width and length direction respectively, as shown in Fig. 1. A distributed transverse load $q(x, y, t)$ is applied to the top surface of composite plate to obtain the transient response. Generally, the variation of a typical volume/weight fraction of CNT in FG-CNTRC structures along the thickness direction is represented by some explicit formulas. But, in this work, the FG-CNT reinforced composite plate is considered to be composed of number of layers (N_L) with equal thickness ($\Delta h = h/N_L$). The effect of CNT reinforcement on dynamic behavior of FG-CNTRC plate is investigated with four different weight fraction distributions (WFD) as shown in Fig. 1. The distribution-I is obtained by considering uniform distribution of weight fraction of CNTs in each layer throughout the thickness and each layer behaves like an isotropic homogenous plate. In distribution-II weight fraction increases from top to mid plane layer and again decreases from mid plane to bottom layer; while distribution-III is reversed case of distribution-II. Distribution-II and distribution-III are symmetric whereas distribution-IV is asymmetric in which weight fraction of CNTs increases linearly from top to bottom layer. More details of these distributions can be found in previous work (Kumar and Srinivas 2017). All these distribution patterns with linear layer-wise variation of weight fractions of CNTs in matrix material are different from the existing formula-based continuous distributions such as uniformly distributed, FG-X etc used earlier.

2.1 Estimation of effective material properties

Basically, multi-walled carbon nanotubes are cylindrical tubes filled with equally spaced concentric walls having internal diameter in the range of 0.4 *nm* to 1 *nm* approximately. For nanocomposites, the empirical relations and rules of mixture cannot predict the mechanical

properties accurately and should be modified as per the experimental or molecular dynamics simulation data. However, the Halpin-Tsai's empirical equation has been recently used in short-fiber reinforced composites with assumption of uniform dispersion and straightness of the fiber.

A modified Halpin-Tsai model is employed here to estimate the effective elastic modulus of the nanocomposite material. The orientation of fiber in polymer matrix decides the effective elastic behavior of composite; despite the CNTs exhibiting the transversely isotropic behavior, the resulting effective properties of randomly oriented CNT reinforced composite are to be considered isotropic. By considering CNTs as an effective cylindrical solid tube with diameter D_{mw}, the effective elastic modulus (E_c) of the randomly oriented CNT reinforced composite is obtained by (Arasteh *et al*. 2011, Rafiee and Firouzbakht 2014, Yeh *et al*. 2006)

$$E_c = \left\{\left(\frac{3}{8}\right)\left[\frac{1+\xi_L\eta_L V_{mw}}{1-\eta_L V_{mw}}\right]+\left(\frac{5}{8}\right)\left[\frac{1+\xi_T\eta_T V_{mw}}{1-\eta_T V_{mw}}\right]\right\}E_p \quad (1)$$

$$\eta_L = \left\{\frac{\left(k_i k_w E_{mw}/E_p\right)-1}{\left(k_i k_w E_{mw}/E_p\right)+\xi_L}\right\},\ \eta_T = \left\{\frac{\left(k_i k_w E_{mw}/E_p\right)-1}{\left(k_i k_w E_{mw}/E_p\right)+\xi_T}\right\} \quad (2)$$

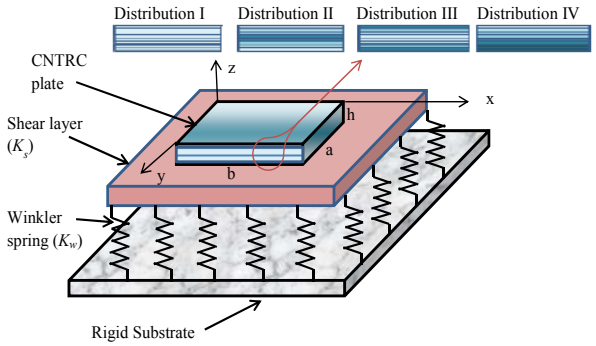

Fig. 1 Schematic depict of multi-layer FG-CNT reinforced composite plate

$$\xi_L = 2\left(\frac{L_{mw}}{D_{mw}}\right)\times k_{agg},\quad \xi_T = 2,\quad k_{agg} = e^{-a_1 V_{mw}-b_1} \quad (3)$$

Density (ρ_c) and Poisson's ratio (υ_c) of nanocomposite material are computed by rule of mixtures according to

$$\upsilon_c = V_{mw}\upsilon_{cnt} + (1-V_{mw})\upsilon_p \quad (4)$$

$$\rho_c = V_{mw}\rho_{cnt} + (1-V_{mw})\rho_p \quad (5)$$

The relationship between the volume fraction (V_{mw}) and weight fraction (w_{mw}) can be expressed as

$$\mathrm{V_{mw}} = \frac{w_{mw}}{[1-(\rho_{mw}/\rho_p)]w_{mw}+(\rho_{mw}/\rho_p)} \quad (6)$$

Here, $()_c$, $()_{mw}$, $()_p$ indicates the properties of composite materials, CNTs and matrix respectively. The length of CNT (L_{mw}) is considered as same as to single walled CNT (L_{cnt}). Also, k_i, k_w and k_{agg} are the factors introduced in conventional Halpin-Tsai model to account the effect of interfacial interaction, waviness and agglomeration in nanocomposites. The constant a_1 and b_1 are related to degree of agglomerates. The effective elastic modulus of CNT (E_{mw}) can be estimated as (Kumar and Srinivas 2017)

$$E_{mw} = \frac{N_w t_{cnt} E_{cnt}}{(N_w-1)h_{in}+t_{cnt}} \quad (7)$$

where t_{cnt} , and E_{cnt} indicate the effective thickness and elastic modulus of single walled CNTs. N_w is number of walls in CNT and h_{in} indicates the inter layer spacing in CNT. The nanotube thickness is considered as 0.141 nm in present analysis (Wang and Zhang 2008). The variation of elastic modulus of CNTs with number of walls and inter layer spacing is depicted in Fig. 2(a) and it is found that N_w = 10, $h_{in} = 1.05\times t_{cnt}$ gives the comparable results (E_{mw} = 950 Gpa) as provided by Yeh *et al*. (2006). The applicability of modified Halpin-Tsai model is supported by available

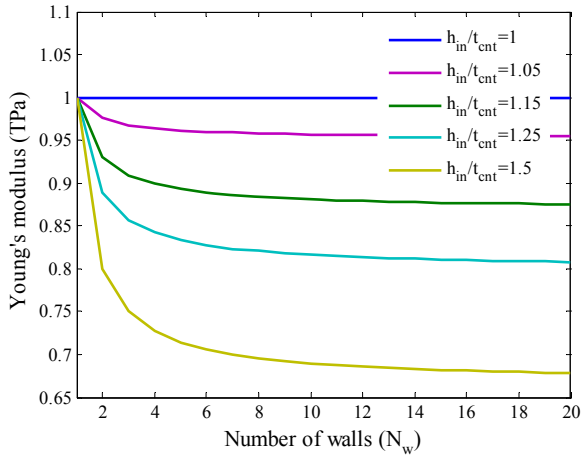

(a) Effective Young's modulus of CNTs (E_{mw})

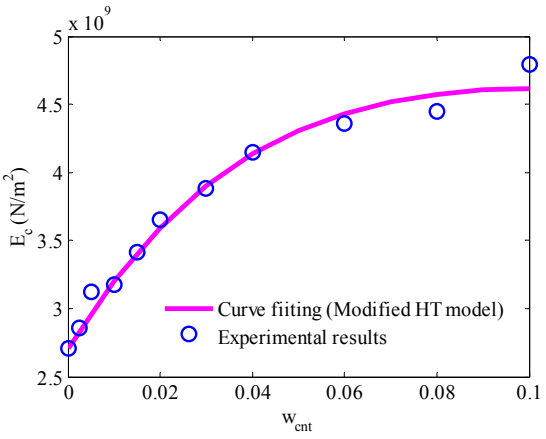

(b) Effective modulus of CNT reinforced composite

Fig. 2 Estimation of effective elastic modulus

experimental data. The effective modulus obtained from present model and experimental results reported by Rafiee and Firouzbakht (2014) are plotted as a function of CNT weight fraction as shown in Fig. 2(b). A similar type of trend is observed for CNT/epoxy composite system. The constant value of parameters in the modified Halpin-Tsai model are obtained from the curve fitting and model parameters related to best fit are $k_i = 0.9694$, $k_w = 0.67$, $a_1 = 18$, $b_1 = 3.4$, $L_{mw} = 75\ \mu$m, $D_{mw} = 70$ nm. These model parameters are further utilized in dynamic solution of nanocomposite plate.

2.2 System of governing equations

Based on higher-order shear deformation theory, in-plane displacement components are linear functions of thickness coordinate whereas out-of-plane components are constant across the thickness. Accordingly, the displacement fields along x, y and z axes is described as

$$\begin{Bmatrix} u(x,y,z,t) \\ v(x,y,z,t) \\ w(x,y,z,t) \end{Bmatrix} = \begin{Bmatrix} u_0(x,y,t) \\ v_0(x,y,t) \\ w_0(x,y,t) \end{Bmatrix} + z \begin{Bmatrix} -\dfrac{\partial w_0(x,y,t)}{\partial x} \\ -\dfrac{\partial w_0(x,y,t)}{\partial y} \\ 0 \end{Bmatrix} + \psi(z) \begin{Bmatrix} \phi_x(x,y,t) \\ \phi_y(x,y,t) \\ 0 \end{Bmatrix} \tag{8}$$

where the terms with subscript $()_0$ indicate the mid surface displacements and ϕ_x and ϕ_y are transverse normal rotations about y and x axes. The term $\psi(z)$ is an appropriate shape function in terms of thickness coordinate which can be easily adapted in various higher order plate theories. In third order shear deformation plate theory $\psi(z) = z - \dfrac{4z^3}{3h^2}$. The strain-displacement relations can be expressed as

$$\varepsilon_b = \begin{Bmatrix} \dfrac{\partial u_0}{\partial x} \\ \dfrac{\partial v_0}{\partial y} \\ \dfrac{\partial u_0}{\partial y} + \dfrac{\partial v_0}{\partial x} \end{Bmatrix} + z \begin{Bmatrix} -\dfrac{\partial^2 w_0}{\partial x^2} \\ -\dfrac{\partial^2 w_0}{\partial y^2} \\ -2\dfrac{\partial^2 w_0}{\partial x \partial y} \end{Bmatrix} + \psi(z) \begin{Bmatrix} \dfrac{\partial \phi_x}{\partial x} \\ \dfrac{\partial \phi_y}{\partial y} \\ \dfrac{\partial \phi_x}{\partial y} + \dfrac{\partial \phi_y}{\partial x} \end{Bmatrix} \tag{9}$$

$$\varepsilon_s = \frac{\partial \psi(z)}{\partial z} \begin{Bmatrix} \phi_y \\ \phi_x \end{Bmatrix} \tag{10}$$

where $\varepsilon_b = \{\varepsilon_{xx}\ \varepsilon_{yy}\ \gamma_{xy}\}^T$ and $\varepsilon_s = \{\gamma_{xz}\ \gamma_{yz}\}^T$ are the bending and shear strain vectors. The expressions for stress component of the k^{th} layer can be obtained by constitutive relations as

$$\begin{Bmatrix} \sigma_b \\ \sigma_s \end{Bmatrix}^{(k)} = \begin{bmatrix} P & 0 \\ 0 & Q \end{bmatrix}^{(k)} \begin{Bmatrix} \varepsilon_b \\ \varepsilon_s \end{Bmatrix}^{(k)} \tag{11}$$

where $\sigma_b = \{\sigma_{xx}\ \sigma_{yy}\ \sigma_{xy}\}^T$, $\sigma_s = \{\sigma_{xz}\ \sigma_{yz}\}^T$ and the non-zero bending and shear stiffness components in matrices P and Q are

$$P_{11}^{(k)} = P_{22}^{(k)} = \frac{E_c^{(k)}}{1-\upsilon_c^2}, \quad P_{12}^{(k)} = P_{21}^{(k)} = \frac{\upsilon_c E_c^{(k)}}{1-\upsilon_c^2}, \quad Q_{11}^{(k)} = Q_{22}^{(k)} = P_{33}^{(k)} = \frac{E_c^{(k)}}{2(1+\upsilon_c)} \tag{12}$$

To obtain the governing equations of motion of composite plate resting on the Pasternak foundation, the Hamilton's principle is employed. That is

$$\int_0^t \left(\delta U + \delta U_{Pf} + \delta W - \delta K\right) dt = 0 \tag{13}$$

where δU, δU_{Pf}, δW and δK are the virtual variation of strain energy, potential energy of Pasternak foundation, work done by external forces and kinetic energy respectively. Also, t is the time required for integration. Detailed expressions of each of the energy functions are

$$\delta U = \int_{-h/2}^{h/2} \int_A \left(\sigma_b \varepsilon_b + \sigma_s \varepsilon_s\right) dA dz \tag{14}$$

$$\delta U_{Pf} = \int_A K_w w_0 \delta w_0 + K_s \left(\frac{\partial w_0}{\partial x}\frac{\partial \delta w_0}{\partial x} + \frac{\partial w_0}{\partial y}\frac{\partial \delta w_0}{\partial y} \right) dx dy \tag{15}$$

where K_w and K_s are the foundation spring constants for Winkler and shear layer. They are obtained as (Wattanasakulpong and Chaikittiratana 2015)

$$K_w = \frac{\beta_w D_0}{a^4}, \quad K_s = \frac{\beta_s D_0}{a^2}, \quad \text{with} \quad D_0 = \frac{E_p h^3}{12(1-\upsilon_p^2)} \tag{16}$$

where β_w and β_s are the foundation stiffness parameters. Similarly, the expressions for kinetic energy and work done by external force are given by

$$\delta K = \int_V \left[\dot{u}\delta\dot{u} + \dot{v}\delta\dot{v} + \dot{w}\delta\dot{w}\right] dx dy dz \tag{17}$$

$$\delta W = -\int_A q \delta w_0 dx dy \tag{18}$$

Finally, the system of governing equations is obtained by subtitling the above energy expressions into Eq. (13) and then applying integration. The resulting coefficients of δu_0, δv_0, δw_0, $\delta\phi_x$ and $\delta\phi_y$ are summarized as

$$\delta u_0: \quad \frac{\partial N_{xx}}{\partial x} + \frac{\partial N_{xy}}{\partial y} = I_1 \ddot{u}_0 - I_2 \frac{\partial \ddot{w}_0}{\partial x} + I_4 \ddot{\phi}_x \tag{19a}$$

$$\delta v_0: \quad \frac{\partial N_{yy}}{\partial y}+\frac{\partial N_{xy}}{\partial x}=I_1\ddot{u}_0-I_2\frac{\partial \ddot{w}_0}{\partial y}+I_4\ddot{\phi}_y \tag{19b}$$

$$\begin{aligned}\delta w_0: \quad & \frac{\partial^2 M_{xx}}{\partial x^2}+\frac{\partial^2 M_{yy}}{\partial y^2}+2\frac{\partial^2 M_{xy}}{\partial x\partial y}-K_w w_0 \\ & +K_s\left(\frac{\partial^2 w_0}{\partial x^2}+\frac{\partial^2 w_0}{\partial y^2}\right)+q(x,y,t)=I_1\ddot{w}_0 \\ & +I_2\left(\frac{\partial \ddot{u}_0}{\partial x}+\frac{\partial \ddot{v}_0}{\partial y}\right)-I_3\left(\frac{\partial^2 \ddot{w}}{\partial x^2}+\frac{\partial^2 \ddot{w}}{\partial y^2}\right)+I_5\left(\frac{\partial \ddot{\phi}_x}{\partial x}+\frac{\partial \ddot{\phi}_y}{\partial y}\right)\end{aligned} \tag{19c}$$

$$\delta\phi_x: \quad \frac{\partial N_{xx}}{\partial x}+\frac{\partial N_{xy}}{\partial y}=I_1\ddot{u}_0-I_2\frac{\partial \ddot{w}_0}{\partial x}+I_4\ddot{\phi}_x \tag{19d}$$

$$\delta\phi_y: \quad \frac{\partial P_{yy}}{\partial y}+\frac{\partial P_{xy}}{\partial x}-R_{yz}=I_4\ddot{u}_0-I_5\frac{\partial \ddot{w}_0}{\partial y}+I_6\ddot{\phi}_y \tag{19e}$$

where I_i (i = 2,….,6) are the mass inertia terms which are defined by

$$\left[I_1,I_2,I_3,I_4,\right]=\sum_{k=1}^{N_L}\int_{Z_k}^{Z_{k+1}}{\rho_c}^k(z)\begin{bmatrix}1,z,z^2,\psi(z),\\ z\psi(z),\psi^2(z)\end{bmatrix}dz \tag{20}$$

in which ${\rho_c}^k$ is the mass density of composite in the k^{th} layer. The normal forces, shear forces, bending moments and their higher order components, which are resulting from constitutive relations of stress in the form of material stiffness and displacement fields, can be written as follows

$$\begin{Bmatrix}N_{xx}\\N_{yy}\\N_{xy}\end{Bmatrix}=[A]\begin{Bmatrix}\frac{\partial u_0}{\partial x}\\ \frac{\partial v_0}{\partial y}\\ \frac{\partial u_0}{\partial y}+\frac{\partial v_0}{\partial x}\end{Bmatrix}+[B]\begin{Bmatrix}-\frac{\partial^2 w_0}{\partial x^2}\\ -\frac{\partial^2 w_0}{\partial y^2}\\ -2\frac{\partial^2 w_0}{\partial x\partial y}\end{Bmatrix}+[C]\begin{Bmatrix}\frac{\partial \phi_x}{\partial x}\\ \frac{\partial \phi_y}{\partial y}\\ \frac{\partial \phi_x}{\partial y}+\frac{\partial \phi_y}{\partial x}\end{Bmatrix} \tag{21}$$

$$\begin{Bmatrix}M_{xx}\\M_{yy}\\M_{xy}\end{Bmatrix}=[B]\begin{Bmatrix}\frac{\partial u_0}{\partial x}\\ \frac{\partial v_0}{\partial y}\\ \frac{\partial u_0}{\partial y}+\frac{\partial v_0}{\partial x}\end{Bmatrix}+[D]\begin{Bmatrix}-\frac{\partial^2 w_0}{\partial x^2}\\ -\frac{\partial^2 w_0}{\partial y^2}\\ -2\frac{\partial^2 w_0}{\partial x\partial y}\end{Bmatrix}+[E]\begin{Bmatrix}\frac{\partial \phi_x}{\partial x}\\ \frac{\partial \phi_y}{\partial y}\\ \frac{\partial \phi_x}{\partial y}+\frac{\partial \phi_y}{\partial x}\end{Bmatrix} \tag{22}$$

$$\begin{Bmatrix}P_{xx}\\P_{yy}\\P_{xy}\end{Bmatrix}=[C]\begin{Bmatrix}\frac{\partial u_0}{\partial x}\\ \frac{\partial v_0}{\partial y}\\ \frac{\partial u_0}{\partial y}+\frac{\partial v_0}{\partial x}\end{Bmatrix}+[E]\begin{Bmatrix}-\frac{\partial^2 w_0}{\partial x^2}\\ -\frac{\partial^2 w_0}{\partial y^2}\\ -2\frac{\partial^2 w_0}{\partial x\partial y}\end{Bmatrix}+[F]\begin{Bmatrix}\frac{\partial \phi_x}{\partial x}\\ \frac{\partial \phi_y}{\partial y}\\ \frac{\partial \phi_x}{\partial y}+\frac{\partial \phi_y}{\partial x}\end{Bmatrix} \tag{23}$$

$$\begin{Bmatrix}R_{yz}\\R_{xz}\end{Bmatrix}=[H]\begin{Bmatrix}\phi_y\\\phi_x\end{Bmatrix} \tag{24}$$

where A_{ij}, B_{ij}, C_{ij}, E_{ij}, F_{ij} and H_{ij} are the stiffness matrices for higher order shear deformation model. The elements of stiffness matrices of the FG-CNTRC plate can be defined as

$$\begin{bmatrix}A_{ij},B_{ij},C_{ij},D_{ij},\\ E_{ij},F_{ij}\end{bmatrix}=\sum_{k=1}^{N_L}\int_{z_k}^{z_{k+1}}P_{ij}^k\begin{bmatrix}1,z,\psi(z),z^2,\\ z\psi(z),\psi^2(z)\end{bmatrix}dz, \quad i,j=1,2,6 \tag{25}$$

$$\left[H_{ij}\right]=\sum_{k=1}^{N_L}\int_{z_k}^{z_{k+1}}\left(\frac{\partial\psi(z)}{\partial z}\right)^2Q_{ij}^k dz, \qquad i=j=4,5 \tag{26}$$

2.3 Approximate solution

Navier method is employed to formulate the closed form dynamic solution of the composite plate with simply supported boundary conditions. By considering the following admissible displacement functions (u_0, v_0, w_0, ϕ_x, and ϕ_y) satisfying the boundary conditions, further analysis is taken up.

$$\begin{Bmatrix}u_0(x,y,t)\\ v_0(x,y,t)\\ w_0(x,y,t)\\ \phi_x(x,y,t)\\ \phi_y(x,y,t)\end{Bmatrix}=\sum_{M=1,3,5....}^{\infty}\sum_{N=1,3,5....}^{\infty}\begin{Bmatrix}u_{mn}(t)\cos\alpha x\sin\beta y\\ v_{mn}(t)\sin\alpha x\cos\beta y\\ w_{mn}(t)\sin\alpha x\sin\beta y\\ \varphi_{mn}(t)\cos\alpha x\sin\beta y\\ \theta_{mn}(t)\sin\alpha x\cos\beta y\end{Bmatrix} \tag{27}$$

where $u_{mn}(t)$, $v_{mn}(t)$, $w_{mn}(t)$, $\varphi_{mn}(t)$ and $\theta_{mn}(t)$ are the arbitrary time dependent constant parameters to be determined. Also, $\alpha = M\pi/a$, $\beta = N\pi$/b and $i=\sqrt{-1}$. The mathematical representation of distributed load is as follows

$$q(x,y,t)=\sum_{M=1}^{\infty}\sum_{N=1}^{\infty}Q_{MN}\sin\alpha x\sin\beta y\times F(t) \tag{28}$$

where

$$Q_{MN}=\frac{4}{ab}\int_0^a\int_0^b q(x,y)\sin\alpha x\sin\beta y dxdy \tag{29}$$

and $F(t)$ is a time dependent function. The exact value of Q_{MN} and $F(t)$ for uniformly distributed load in terms of pulse duration can be defined as (Kazanci 2009, Wang *et al*. 2001)

$$Q_{MN}=\frac{16q_0}{MN\pi^2} \quad (M=N=1,3,5....) \tag{30}$$

$$F(t)=\begin{cases}t/t_p \ \ if\ 0\le t\le t_p\\ 0 \ \ if\ t>t_p\end{cases} \quad \text{for triangular pulse} \tag{31a}$$

$$=\begin{cases}\sin\left(\frac{\pi t}{t_p}\right) \ \ if\ 0\le t\le t_p\\ 0 \ \ if\ t>t_p\end{cases} \quad \text{for sinusoidal pulse} \tag{31b}$$

$$= \begin{cases} 1 \ \ if \ \ 0 \le t \le t_p \\ 0 \ \ if \ \ t > t_p \end{cases} \quad \text{for rectangular pulse} \tag{31c}$$

$$= \left(1 - \frac{t}{t_p}\right) e^{-\varphi t / t_p} \quad \text{for explosive blast pulse} \tag{31d}$$

where q_0 and t_p are the peak value of the distributed load and duration of the pulse. It is presumed that peak value of the load is q_0 = -100 *kPa* and pulse duration t_p is 0.0005 s. Also, φ is a waveform parameters in blast loading taken as 0.35 (Kazanci 2009).

After substituting Eqs. (27) and (28) into Eq. (19), a set of time dependent algebraic equations are derived as

$$[M]\ddot{\Delta}(t) + [K]\Delta(t) = Q(t) \tag{32}$$

where [K], and [M] are the overall stiffness, and mass matrices of size 5×5, $\Delta(t)$ is the unknown displacement vector while $Q(t)$ is the force vector respectively, which are given as

$$\Delta(t) = \begin{Bmatrix} u_{mn}(t) \\ v_{mn}(t) \\ w_{mn}(t) \\ \varphi_{mn}(t) \\ \theta_{mn}(t) \end{Bmatrix}, \qquad Q(t) = \begin{Bmatrix} 0 \\ 0 \\ Q_{MN} F(t) \\ 0 \\ 0 \end{Bmatrix} \tag{33}$$

In present analysis the damping matrix [C] is computed according to as [C] = $\{2c/\omega_1\}[K]$ (Ansari and Gholami 2016, Ansari *et al*. 2015), where ω_1 is the fundamental natural frequency of the system and c is a damping coefficient. The non-conservative damping forces [C] $\dot{\Delta}(t)$ is introduced in Eq. (32) and final governing equation becomes

$$[M]\ddot{\Delta}(t) + [C]\dot{\Delta}(t) + [K]\Delta(t) = Q(t) \tag{34}$$

3. Numerical illustrations

A detailed numerical study is presented in this work for transient vibration analysis of multi-layer functionally graded CNT-reinforced polymer composite plate. The equations of motion are solved by fourth order Runge-Kutta method with zero initial conditions.

First, the convergence study is carried out by considering different number of layers in plate to confirm the stability and accuracy of present solution. A dimensionless central deflection $\left(\overline{w} = \frac{D_0 w(a/2, b/2) \times 10^3}{a^4 q_0}\right)$ is obtained under triangular pulse load for the distribution-III by varying the number of layers in thickness direction. Fig. 3(a) shows the consistency in results for 8 to 10 layers (N_L) in composite plate without elastic foundation. Also, an illustration for validate the results and investigate the effect of number of terms in the Fourier expression of displacement functions is presented. In which, central deflection (w) of the isotropic plate under sudden dynamic load is computed according to the dimensions and material properties of the previous work (Lei *et al*. 2015). It can be observed from Fig. 3(b) that one term solution is sufficient to yield converged results. For further analysis, multi-layer functionally graded CNT reinforced nanocomposite plate with simply supported boundary conditions is considered. Table 1 shows the material properties employed in the simulations. The weight fraction of CNTs is considered as 1% and N_L = 10 throughout the analysis. A parallel solution of composite plate is obtained from finite element analysis using ANSYS 15.0 with SHELL-281 elements (8-node,

Table 1 Material properties and model parameters for CNT reinforced composite

Polymer (epoxy)	CNTs
$E_p = 2.71$ *GPa* $\rho_p = 1300$ kg/m^3 $\upsilon_p = 0.3$	$E_{mw} = 950$ *GPa*, $\upsilon_{mw} = 0.28$, $\rho_{mw} = 1180$ *kg*/m^3, $L_{mw} = 75$ *μm*, $D_{mw} = 70$ *nm*, $k_i = 0.9694$, $k_w = 0.67$, $a_1 = 18$, $b_1 = 3.4$

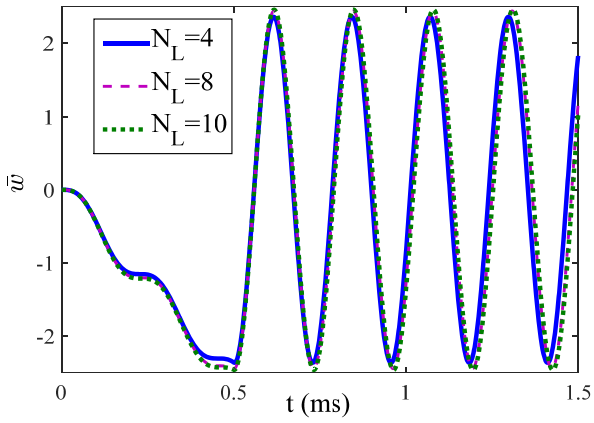

(a) FG-CNTRC Plate ($\beta_w = \beta_s = 0$, $M = N = 1$, $a/h = 10$, $w_{mw} = 1\%$)

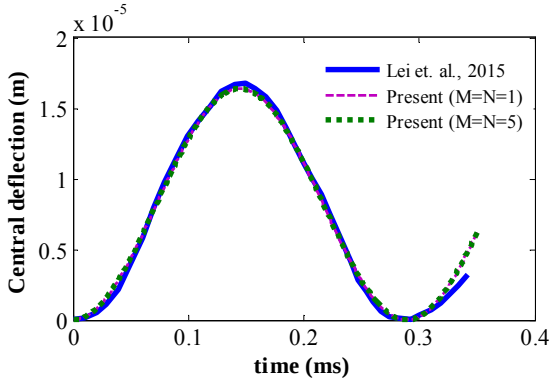

(b) Isotropic plate

Fig. 3 Dimensionless central deflection response of plate

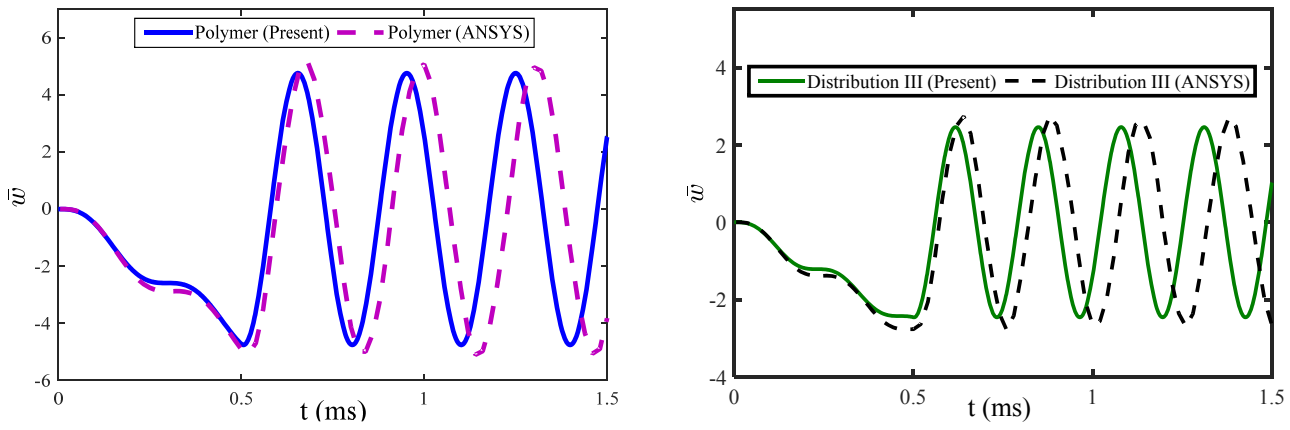

(a) Polymer plate (b) FG-CNTRC plate

Fig. 4 Comparison for dimensionless central deflection response ($\beta_w = \beta_s = 0$, $a/h = 10$, $w_{mw} = 1\%$)

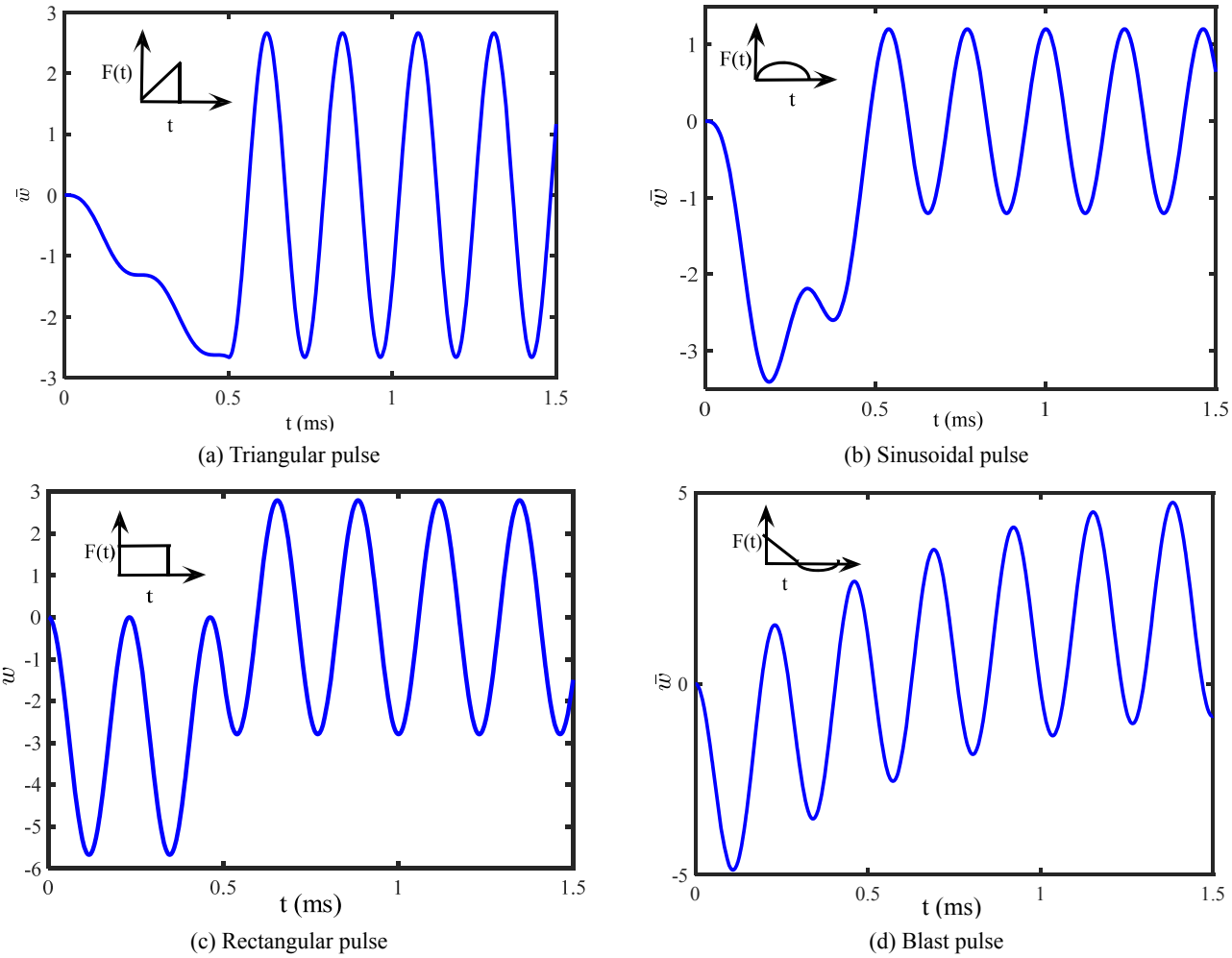

(a) Triangular pulse (b) Sinusoidal pulse

(c) Rectangular pulse (d) Blast pulse

Fig. 5 FG-CNT reinforced composite plate under different loading conditions ($\beta_w = 100$, $\beta_s = 0$, $a/h = 10$, $w_{mw} = 1\%$, distribution III)

6 degree of freedom per node). The plate is assumed to be composed of 10 layers with each layer property computed according to functional grading concept. After several trails, it was found that 20×20 mesh size is enough to get converge and reliable results. Fig. 4 shows numerical results for simply supported plate without elastic foundation in comparison with the ANSYS results of pure polymer and distribution III. It can be seen that the results are close to each other.

Fig. 5 shows the response of FG-CNT reinforced composite plate due to different types of loads. It is observed that the responses become steady immediately

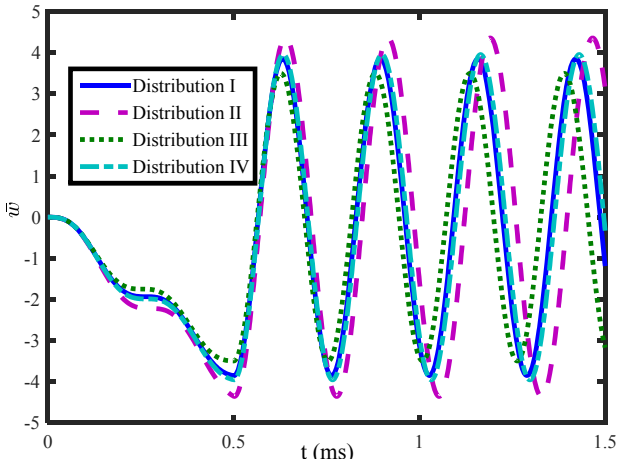

Fig. 6 FG-CNTRC plate response for different distributions ($\beta_w = 0$, $\beta_s = 0$, $a/h = 10$, $w_{mw} = 1\%$)

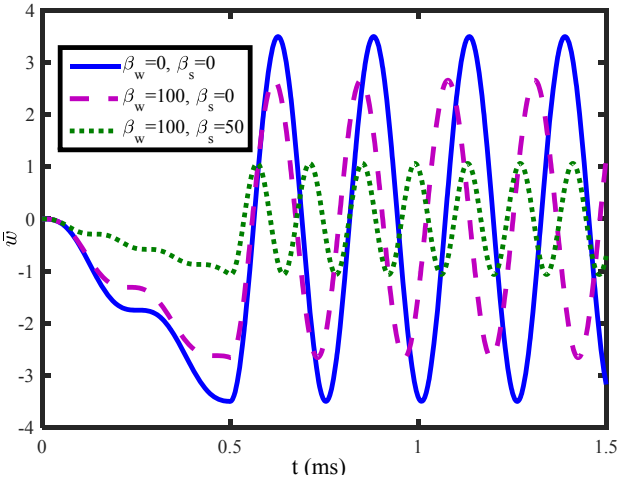

Fig. 7 FG-CNTRC plate response with elastic foundation parameters ($a/h = 10$, $w_{mw} = 1\%$, distribution III)

after the loading duration in first three cases. Most of the available work in literature deals with rectangle, sinusoidal, decreasing type of triangular and blast loadings. So, in present work, further analysis of composite plate behavior is carried out with increasing type of triangular loading. Fig. 6 depicts the behavior of dimensionless central deflection response of simply supported FG-CNT reinforced composite plate for different types of distributions. Here, the triangular pulse load is considered. Distribution-II shows the highest central deflection while the distribution-III gives the minimum central deflection. Fig. 7 depicts the effect of elastic foundation stiffness on the response of FG-CNT reinforced composite plate for distribution- III. Increasing the elastic foundation coefficient drastically decreases the central deflection. Now, the effect of weight fraction and aspect ratio of CNTs are investigated. Fig. 8 shows the central response of polymer plate along with that of composite plates with two different weight fractions. It is discerned from figure that as the weight fraction increases, response amplitudes decrease. In other words, stiffening effect becomes more pronounced for higher weight fractions. It can be understood from Fig. 9 that long CNTs

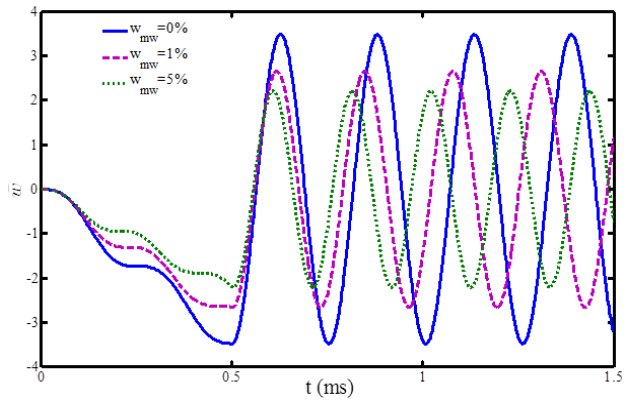

Fig. 8 FG-CNTRC plate response with variation of weight fraction ($\beta_w = 100$, $\beta_s = 0$, $a/h = 10$, Distribution III)

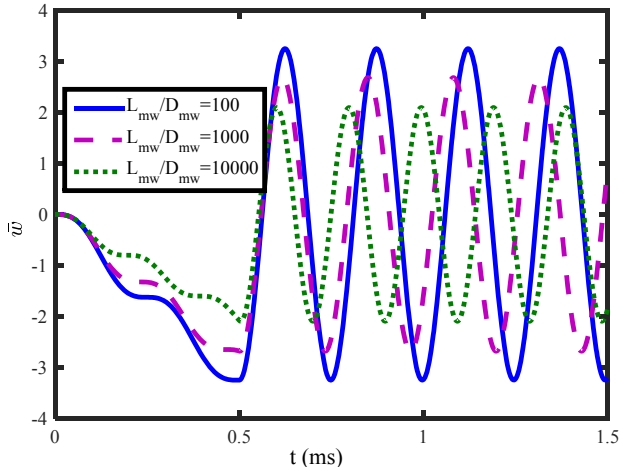

Fig. 9 FG-CNTRC plate response with CNT aspect ratio ($\beta_w = 100$, $\beta_s = 0$, $a/h = 10$, $w_{mw} = 1\%$, distribution III)

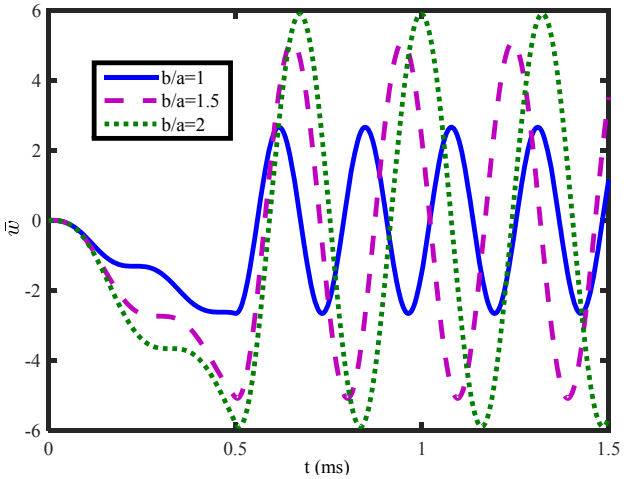

Fig. 10 FG-CNTRC plate response with plate aspect ratio ($\beta_w = 100$, $\beta_s = 0$, $a/h = 10$, $w_{mw} = 1\%$, distribution III)

provide good reinforcing capability resulting in higher stiffness which in turn reduces central deflection amplitude. Fig. 10 shows the dimensionless central deflection history for three different plate aspect ratios. It is observed that

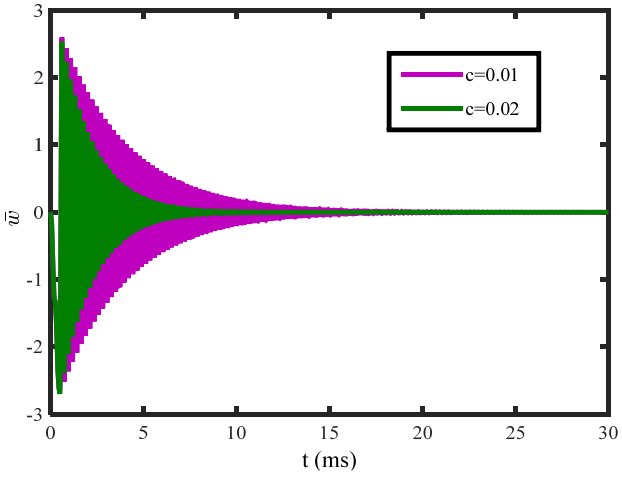

Fig. 11 Effect of damping coefficient on transient response of FG-CNTRC plate (β_w = 100, β_s = 0, distribution III, w_{mw} = 1%)

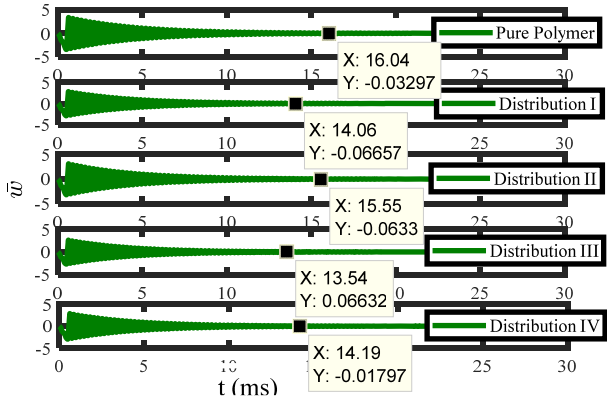

Fig. 12 Transient response of FG-CNTRC plate (β_w = 100, β_s = 0, w_{mw} = 1%, a/h = 10, c = 0.01)

square plate shows lower central deflections as compared to rectangle one.

In Fig. 11, the effect of damping coefficient on non-dimensional central deflection is investigated and it is observed that increment in the damping coefficient reduces the settling time. Fig. 12 shows the effect of weight fraction distributions on settling time of nanocomposite plate. It is observed from data point that composite plate with distribution-III takes minimum time (x-coordinate) to attain rest position, while pure polymer plate takes maximum time. Despite of distribution II and III are symmetric, distribution II shows the opposite behavior to distribution III and takes maximum settling time among all distributions.

4. Conclusions

Transient vibration studies of functionally graded CNTs reinforced composite simply-supported plate with Pasternak foundation have been presented. Layer-wise theory was implemented for analyzing the functionally graded distribution in the thickness direction. The plate was viewed as an assemblage of perfectly bonded finite thickness thin layers and each layer consist of uniform distributed of CNTs. The weight fractions of CNTs in layers were varied in such a way that it can achieve the CNT distribution as per functional grading concept. By considering multi-walled carbon nanotube as reinforcement, the elastic properties of composite plate were estimated using modified Halpin-Tsai model. Equations of motion were derived by considering shear deformation effects and proportional damping. The transient solution was obtained by employing Navier's solution technique along with the explicit time integration scheme. The results showed that composite plate behaves differently under various time dependent pulse excitation. This may helpful to design the composite structures under different loading conditions. In light of the triangular pulse, obtained numerical outcomes are presented as some important conclusions.

- Slight increase in CNT weight fraction diminishes the central vertical deflection of composite plate.
- Higher aspect ratio of CNTs resulting in to low response amplitudes.
- Distribution-III is relatively better as it gives the lowest central deflection.
- At higher plate aspect ratio, the central deflection increases rapidly while a significant decrement is observed in central deflection with elastic foundation.
- Minimum settling time is observed for distribution III compared to other four distributions.

As a future scope of the work, an experimental analysis has to be carried-out to confirm the effects of primary factors like weight fractions and plate geometry on the transient response behavior. The type of distribution and material optimization of CNT reinforced composite is another goal. The influence of structural damping may be studied under impact loads.

Acknowledgments

The authors are thankful to National Institute of Technology Rourkela for providing computational facilities and infrastructure to carry out the research work.

References

Ansari, R. and Gholami, R. (2016), "Nonlinear primary resonance of third-order shear deformable functionally graded nanocomposite rectangular plates reinforced by carbon nanotubes", *Compos. Struct.*, **154**, 707-723.

Ansari, R., Hasrati, E., Faghih Shojaei, M., Gholami, R. and Shahabodini, A. (2015), "Forced vibration analysis of functionally graded carbon nanotube-reinforced composite plates using a numerical strategy", *Phys. E: Low-Dimens. Syst. Nanostruct.*, **69**, 294-305.

Arasteh, R., Omidi, M., Rousta, A.H.A. and Kazerooni, H. (2011), "A study on effect of waviness on mechanical properties of multi-walled carbon nanotube/epoxy composites using modified Halpin–Tsai theory", *J. Macromol. Sci. Part B*, **50**(12), 2464-2480.

Bayat, M.R., Rahmani, O. and Mosavi Mashhadi, M. (2016), "Nonlinear low-velocity impact analysis of functionally graded nanotube-reinforced composite cylindrical shells in thermal environments", *Polym. Compos.*, **39**(3), 730-745. DOI: 10.1002/pc.23990

Chavan, S.G. and Lal, A. (2017), "Bending behavior of SWCNT reinforced composite plates", *Steel Compos. Struct., Int. J.*, **24**(5), 537-548.

Ebrahimi, F. and Habibi, S. (2017), "Low-velocity impact response of laminated FG-CNT reinforced composite plates in thermal environment", *Adv. Nano Res., Int. J.*, **5**(2), 69-97.

Feng, C., Kitipornchai, S. and Yang, J. (2017), "Nonlinear free vibration of functionally graded polymer composite beams reinforced with graphene nanoplatelets (GPLs)", *Eng. Struct.*, **140**, 110-119.

Guo, X.Y. and Zhang, W. (2016), "Nonlinear vibrations of a reinforced composite plate with carbon nanotubes", *Compos. Struct.*, **135**, 96-108. DOI: https://doi.org/10.1016/j.compstruct.2015.08.063

Hao, Y.X., Zhang, W. and Ji, X.L. (2010), "Nonlinear dynamic response of functionally graded rectangular plates under different internal resonances", *Math. Probl. Eng.*, **2010**, 738648-1-12.

Jangam, S., Raja, S. and Maheswar Gowd, B.U. (2016), "Influence of multiwall carbon nanotube alignment on vibration damping of nanocomposites", *J. Reinf. Plast. Compos.*, **35**(8), 617-627.

Kazanci, Z. (2009), "Nonlinear transient response of a laminated composite plate under time-dependent pulses", *Int. Conf. Recent Adv. Sp. Technol.*, **4**, 125-130.

Kumar, P. and Srinivas, J. (2014), "Numerical evaluation of effective elastic properties of CNT-reinforced polymers for interphase effects", *Comput. Mater. Sci.*, **88**, 139-144.

Kumar, P. and Srinivas, J. (2017), "Vibration, buckling and bending behavior of functionally graded multi-walled carbon nanotube reinforced polymer composite plates using the layer-wise formulation", *Compos. Struct.*, **177**, 158-170.

Kumar, D. and Srivastava, A. (2016), "Elastic properties of CNT - and graphene - reinforced nanocomposites using RVE", *Steel Compos. Struct., Int. J.*, **21**(5), 1085-1103.

Lei, Z.X., Zhang, L.W. and Liew, K.M. (2015), "Elastodynamic analysis of carbon nanotube-reinforced functionally graded plates", *Int. J. Mech. Sci.*, **99**, 208-217.

Malekzadeh, P. and Monajjemzadeh, S.M. (2013), "Dynamic response of functionally graded plates in thermal environment under moving load", *Compos. Part B: Eng.*, **45**(1), 1521-1533.

Moradi-Dastjerdi, R. and Momeni-Khabisi, H. (2018), "Vibrational behavior of sandwich plates with functionally graded wavy carbon nanotube-reinforced face sheets resting on Pasternak elastic foundation", *J. Vib. Control*, **24**(11), 2327-2343.

Najafi, F., Shojaeefard, M.H. and Saeidi Googarchin, H. (2016), "Nonlinear low-velocity impact response of functionally graded plate with nonlinear three-parameter elastic foundation in thermal field", *Compos. Part B: Eng.*, **107**, 123-140.

Phung-Van, P., Nguyen, L.B., Tran, L.V., Dinh, T.D., Thai, C.H., Bordas, S.P.A., Abdel-Wahab, M. and Nguyen-Xuan, H. (2015), "An efficient computational approach for control of nonlinear transient responses of smart piezoelectric composite plates", *Int. J. Non-Linear Mech.*, **76**, 190-202.

Phung-Van, P., Ferreira, A.J.M., Nguyen-Xuan, H. and Abdel Wahab, M. (2017a), "An isogeometric approach for size-dependent geometrically nonlinear transient analysis of functionally graded nanoplates", *Compos. Part B: Eng.*, **118**, 125-134.

Phung-Van, P., Tran, L.V., Ferreira, A.J.M., Nguyen-Xuan, H. and Abdel-Wahab, M. (2017b), "Nonlinear transient isogeometric analysis of smart piezoelectric functionally graded material plates based on generalized shear deformation theory under thermo-electro-mechanical loads", *Nonlinear Dyn.*, **87**(2), 879-894.

Rafiee, R. and Firouzbakht, V. (2014), "Multi-scale modeling of carbon nanotube reinforced polymers using irregular tessellation technique", *Mech. Mater.*, **78**, 74-84.

Seidel, G.D. and Lagoudas, D.C. (2006), "Micromechanical analysis of the effective elastic properties of carbon nanotube reinforced composites", *Mech. Mater.*, **38(**8-10), 884-907.

Sharma, A., Kumar, A., Susheel, C.K. and Kumar, R. (2016), "Smart damping of functionally graded nanotube reinforced composite rectangular plates", *Compos. Struct.*, **155**, 29-44.

Shokravi, M. (2017), "Buckling of sandwich plates with FG-CNT-reinforced layers resting on orthotropic elastic medium using Reddy plate theory", *Steel Compos. Struct., Int. J.*, **23**(6), 623-631.

Song, M., Kitipornchai, S. and Yang, J. (2017), "Free and forced vibrations of functionally graded polymer composite plates reinforced with graphene nanoplatelets", *Compos. Struct.*, **159**, 579-588.

Swain, A., Roy, T. and Nanda, B.K. (2017), "Vibration damping characteristics of carbon nanotubes-based thin hybrid composite spherical shell structures", *Mech. Adv. Mater. Struct.*, **24**(2), 95-113.

Tahouneh, V. (2017), "Using modified Halpin-Tsai approach for vibrational analysis of thick functionally graded multi-walled carbon nanotube plates", *Steel Compos. Struct., Int. J.*, **23**(6), 657-668.

Udupa, G., Rao, S.S. and Gangadharan, K.V. (2012), "Future applications of carbon nanotube reinforced functionally graded composite materials", *Proc. Int. Conf. Adv. Eng. Sci. Manage.*, **1**, 399-404.

Wang, C.Y. and Zhang, L.C. (2008), "A critical assessment of the elastic properties and effective wall thickness of single-walled carbon nanotubes", *Nanotechnology*, **19(**7), 75705-1-5.

Wang, Y.Y., Lam, K.Y. and Liu, G.R. (2001), "A strip element method for the transient analysis of symmetric laminated plates", *Int. J. Solids Struct.*, **38**(2), 241-259.

Wattanasakulpong, N. and Chaikittiratana, A. (2015), "Exact solutions for static and dynamic analyses of carbon nanotube-reinforced composite plates with Pasternak elastic foundation", *Appl. Math. Model.*, **39**(18), 5459-5472.

Yeh, M.-K., Tai, N.-H. and Liu, J.-H. (2006), "Mechanical behavior of phenolic-based composites reinforced with multi-walled carbon nanotubes", *Carbon*, **44**(1), 1-9.

Zhang, L.W., Xiao, L.N., Zou, G.L. and Liew, K.M. (2016), "Elastodynamic analysis of quadrilateral CNT-reinforced functionally graded composite plates using FSDT element-free method", *Compos. Struct.*, **148**, 144-154.

Zhang, L.., Lei, Z.X. and Liew, K.M. (2017), "Free vibration analysis of FG-CNT reinforced composite straight-sided quadrilateral plates resting on elastic foundations using the IMLS-Ritz method", *J. Vib. Control*, **23**(6), 1026-1043.

CC